

Effect of different intraoral scanners and post-space depths on the trueness of digital impressions

Marwa Emam^{1,A–F}, Lomaya Ghanem^{2,B,F}, Hoda M. Abdel Sadek^{1,A–D,F}

¹ Department of Fixed Prosthodontics, Faculty of Dentistry, Ain Shams University, Cairo, Egypt

² Department of Fixed Prosthodontics and Conservative Dentistry, Faculty of Oral and Dental Medicine, Misr International University, Cairo, Egypt

A – research concept and design; B – collection and/or assembly of data; C – data analysis and interpretation;

D – writing the article; E – critical revision of the article; F – final approval of the article

Dental and Medical Problems, ISSN 1644-387X (print), ISSN 2300-9020 (online)

Dent Med Probl. 2024;61(4):577–584

Address for correspondence

Marwa Emam

E-mail: marwaemam@asfd.asu.edu.eg

Funding sources

None declared

Conflict of interest

None declared

Acknowledgements

The authors would like to thank Dr. Yasmine Ashraf for her assistance with the Geomagic® software.

Received on February 24, 2023

Reviewed on March 15, 2023

Accepted on March 23, 2023

Published online on April 18, 2023

Abstract

Background. The trueness of intraoral scanners (IOSs) has been evaluated in many clinical situations. However, the tests of their performance when scanning post-space preparations are still lacking.

Objectives. The aim of the present study was to compare the trueness of the digital impressions of post spaces with different depths, captured by means of different IOSs.

Material and methods. Digital impressions of teeth ($N = 16$) with post spaces of depths of 8 mm and 10 mm were captured. Three IOSs were used, including Primescan AC, Medit i500 and CS 3600. The STL files were compared to the files obtained from the traditional impression scanning performed with an InEos X5 desktop scanner. Then, reverse engineering software measured the trueness values, which were analyzed using the two-way analysis of variance (ANOVA), followed by Tukey's post-hoc test. The significance level was set at $p < 0.05$.

Results. Significant differences were found between the scanners in terms of root mean square (RMS) values ($p < 0.001$). The highest RMS value was found for CS 3600 (0.30 ± 0.11 mm), followed by Primescan AC (0.26 ± 0.09 mm), while the lowest value was found for Medit i500 (0.18 ± 0.05 mm). The 8-millimeter-deep post spaces had a significantly higher RMS value than the 10-millimeter-deep ones (0.28 ± 0.10 mm and 0.21 ± 0.09 mm, respectively) ($p = 0.009$).

Conclusions. The Medit i500 scanner showed the highest post-space digital impression trueness as compared to Primescan AC and CS 3600. In the digital impressions captured with CS 3600, the 10 mm post-space depth had higher trueness than the 8 mm depth. Moreover, CS 3600 was less able to capture the full length of both the 8 mm and 10 mm post-space depths than Primescan AC and Medit i500.

Keywords: CAD/CAM, root canal preparation, scanners, post-and-core technique

Cite as

Emam M, Ghanem L, Abdel Sadek HM. Effect of different intraoral scanners and post-space depths on the trueness of digital impressions. *Dent Med Probl.* 2024;61(4):577–584. doi:10.17219/dmp/162573

DOI

10.17219/dmp/162573

Copyright

Copyright by Author(s)

This is an article distributed under the terms of the Creative Commons Attribution 3.0 Unported License (CC BY 3.0) (<https://creativecommons.org/licenses/by/3.0/>).

Introduction

Most endodontically treated teeth require a core build-up with restorative materials to restore the lost tooth structure, and a post inserted inside the root canal to retain the core.¹ Ideally, the post should be bonded with a thin uniform layer of resin cement. A thick cement layer leads to polymerization contraction and creates internal stresses that cause cement fractures and the debonding of the post.¹ Moreover, root canals may show anomalies that affect the cement layer thickness, though custom-made posts have a shape that is more similar to the actual anatomy of the root canal. Conventionally, customized posts and cores are constructed in a two-step procedure that involves taking an impression, followed by fabrication in the dental laboratory.^{2–5} Conventional impressions are taken with the use of elastomeric impression materials. Indeed, the accuracy and biocompatibility of these materials have been established.⁶ Nonetheless, their use is related to several inconveniences, both from the operator's and the patient's standpoint, as it can cause anxiety, discomfort and nausea.^{5,7}

The launch of computer-aided design and computer-aided manufacturing (CAD/CAM) technologies has revolutionized the processing of dental restorations.⁸ A significant aspect of CAD/CAM are the scanners used, available as intraoral or extraoral devices. An intraoral scanner (IOS) provides direct imaging, while an extraoral scanner provides indirect imaging by scanning the master cast poured from the analog impression.⁹ A digital impression created with IOS can be easily repeated and easily transferred to the dental laboratory, and the process itself is characterized by real-time model visualization and time efficiency.^{7,10–14} However, digital systems have drawbacks, such as the significant cost of the initial purchase and the ongoing maintenance, difficulty in detecting deep margins, and the fact that blood and saliva hinder data capture.¹⁵ Nonetheless, the dimensional accuracy of digital models generated by intraoral scanning is deemed high in comparison with the desktop scanning of conventional impressions.^{16–22}

Conventional impressions can be digitalized for CAD/CAM post and core fabrication after being sprayed with an anti-reflective coating. Furthermore, the introduction of IOS has enabled the direct scanning of intra-canal post-space preparations without the use of conventional impression techniques.^{23,24} Regardless, limitations related to the intraoral environment (oral fluids) and IOS motion, especially in the posterior region, should be taken into consideration.¹

Trueness is defined as 'the ability of a measurement to match the actual value'.^{25,26} The trueness of IOS is affected by the scan pattern, the properties of the scanned object, the distance between the scanner and the object, and the size of the scanner head and lightbox.^{27–32} The three-dimensional (3D) trueness of a virtual model can

be evaluated by calculating its root mean square (RMS) value.³³ The comparative analysis of 3D data can be performed by using a coordinate-measuring machine³⁴ or metrology software,²⁶ which has been adopted from engineering and used to evaluate IOS and conventional impressions.²⁶ Meanwhile, precision is defined as 'the ability of a measurement to be consistently reproduced'.²⁶ Although trueness and precision are independent and each can be assessed separately, when both parameters are measured, they can be used to evaluate the accuracy of IOS.

The ability of different scanners to accurately read the post-space depth is not clear yet. Only a few studies have assessed the effect of the post-space depth on digital and conventional silicon impression accuracy.^{1,35} Therefore, the present study aimed to compare the trueness of the digital impressions of post spaces with different depths, captured by means of different IOSs. The null hypothesis was that trueness would not differ according to the post-space depth or the type of IOS used.

Material and methods

The study was approved by the ethics committee at the Faculty of Dentistry of the Ain Shams University, Cairo, Egypt (FDASU-REC ER032238).

A total of 16 ($N = 16$) single straight-rooted human teeth – maxillary incisors and mandibular premolars – free of cracks and caries were selected. A priori power analysis was performed using the G*Power software, v.3.1.9.7 (<https://www.psychologie.hhu.de/arbeitsgruppen/allgemeine-psychologie-und-arbeitspsychologie/gpower>), based on the results of a previous study.³⁶ The minimum group sample size was determined to be 2 (power = 0.95; effect size = 8.01), and an increase in the group sample size could increase the study power. The sample teeth were collected so that their root anatomy and dimensions would be similar. The teeth were cleaned and stored in distilled water throughout the sampling period before being decoronated by using a diamond disk mounted on a straight handpiece at 2 mm coronal to the cemento-enamel junction and perpendicular to the long axis of the tooth. A routine root canal treatment procedure was carried out and periapical radiographs were used for inspection. The roots were randomly assigned into 2 groups ($n = 8$) according to the depth of post-space drilling, at either 8 mm (group 8) or 10 mm (group 10). Each root was mounted vertically in an acrylic block by using self-cured acrylic resin (Acrostone Dental & Medical Supplies, Cairo, Egypt) (Fig. 1). A single operator prepared standardized post spaces for all teeth by using a tapered post drill #1.6 mm (Olipost Drill, Olident, Cracow, Poland).

Digital and traditional impressions were taken for each sample. Digital impressions were obtained first,

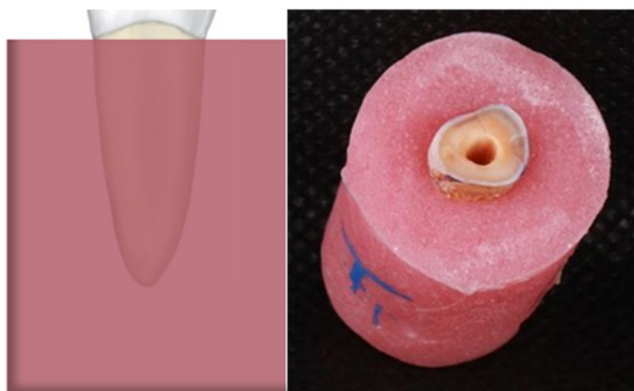


Fig. 1. Diagram and photo of the sample mounted in an acrylic block

as the silicone material remaining after applying the conventional impression technique might affect the post-space depth, and thus the accuracy of the digital impression data. The digital impressions of the post spaces were created with 3 different IOSs, including Primescan AC with Connect™ Software (Dentsply Sirona, Bensheim, Germany), Medit i500 (Medit Corp., Seoul, South Korea) and CS 3600 (Carestream Dental, Stuttgart, Germany). The scanner systems, manufacturers, software versions, and scanning technologies are listed in Table 1.

An occlusal notch was marked buccally as a starting point, the samples were fixed in place and all scanners were rotated clockwise. Digital scanning was performed at room temperature by an experienced operator to minimize operator experience bias.³⁷ STL files were generated from each IOS for all samples. Traditional impressions were taken with polyvinyl siloxane (SwissTEC HydroXtreme; Coltène/Whaledent, Altstätten, Switzerland), using a single-step two-material impression technique (Fig. 2).

To evaluate the trueness of the IOS reference, STL files were created by scanning each impression with an extraoral InEos X5 desktop scanner (Dentsply Sirona, Charlotte, USA), which is a highly accurate laboratory scanner that uses the digital stripe projection scanning technology with blue light, with each impression fixed separately to the five-axis robotic arm of the scanner.

Table 1. Scanner systems, manufacturers, software versions, and scanning technologies of the scanners used in the study

System	Manufacturer	Software	Technology
Primescan AC	Dentsply Sirona, Bensheim, Germany	CEREC 4.5	confocal microscopy
Medit i500	Medit Corp., Seoul, South Korea	Medit Link 2.1.2	dual camera optical triangulation
CS 3600	Carestream Dental, Stuttgart, Germany	CS ScanFlow 1.0.5	active triangulation
InEos X5	Dentsply Sirona, Charlotte, USA	inLab 15	optical blue structured light

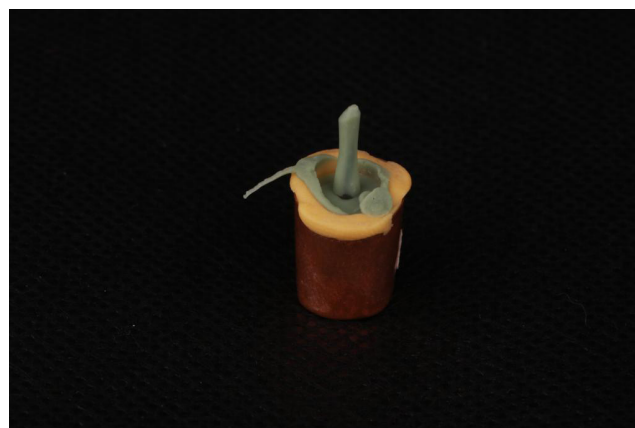


Fig. 2. Polyvinyl siloxane impression of a post space, ready for scanning with a desktop scanner

The trueness of the IOS was evaluated using reverse engineering software (Geomagic® Control X™ 2018; 3D Systems Manufacturing, Rock Hill, USA). The reference standard scan model was first trimmed to remove irrelevant data points and leave only the post-space data, which needed to be aligned. The unnecessary data points were excluded from the comparison with the test scans. Then, the “resegmenting” tool was used to manually segment the reference model, which enabled the restriction of deviation calculations to custom datasets. Each IOS scan file was imported, and then superimposed onto the reference model by using the initial alignment and the best-fit alignment for trueness measurements. The software best-fit alignment algorithm used the iterative closest-point procedure to align the 3D digital data of the test files and the reference files, which is the industry standard. After alignment, the “3D compare” function enabled the automatic isolation and comparison of substrate regions for the deviation computation of all locations of interest in post-space regions. The color-coded photographs of the model revealed the degree and pattern of the deviation of the 3D model. Darker blue signified a negative or inward deviation, while darker red signified a positive or outward deviation of the test model (Fig. 3).

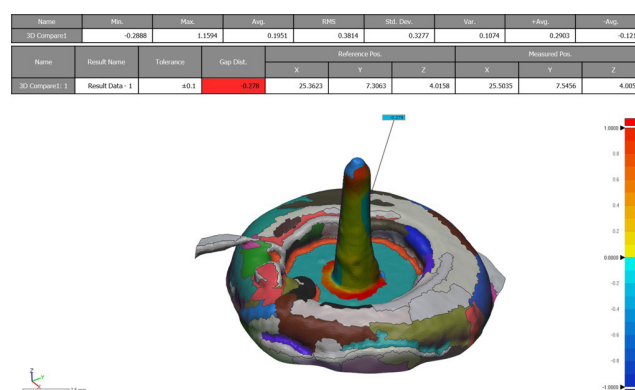


Fig. 3. Three-dimensional (3D) comparison of the superimposed test and reference post scans, showing the color map and the root mean square (RMS) value

Trueness was expressed as RMS, and the square of the phase difference between several points in 3D space was calculated (X-axis, Y-axis and Z-axis). The sum of these squares was then divided by the number of points, and the RMS was calculated as the square root of this value, using the following formula (Equation 1):

$$RMS = \frac{1}{\sqrt{n}} \times \sqrt{\sum_{i=1}^n (x_{1i} - x_{2i})^2} \quad (1)$$

where:

x_{1i} – measurement of point i on the reference scan;

x_{2i} – measurement of point i on the test scan; and

n – total number of points measured in each analysis.

The RMS value may be employed to assess how different from zero the deviation between 2 different sets of data is. The lower the RMS value, the better the 3D agreement of the superimposed data.³³

As for the length measurement with regard to the post-space depth, the STL files of the tested specimens were imported to the software individually before the “2D length measurement” tool was selected. To get the length of the post-space depth captured by each scanner, the distance from the selected point on the occlusal surface (the occlusal notch) to the apical end of the post scan was measured (Fig. 4).

Statistical analysis

Statistical analysis was conducted with the use of the R statistical analysis software, v. 4.1.2 for Windows (R Core Team. R: A language and environment for statistical

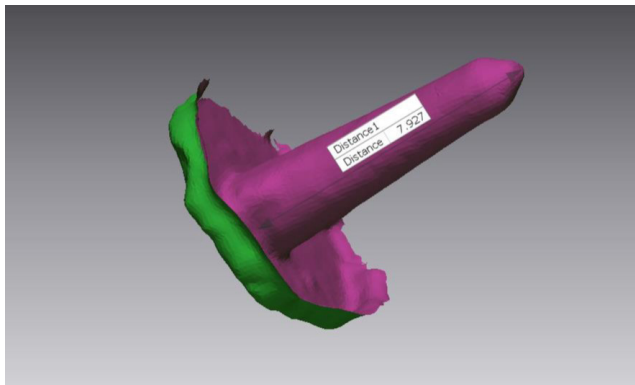


Fig. 4. Measurement of the post-scan length

computing. R Foundation for Statistical Computing, Vienna, Austria). Numerical data was presented as mean and standard deviation ($M \pm SD$). The normality of data was assessed using the Shapiro–Wilk test, and Levene’s test determined the homogeneity of variance. The data showed a parametric distribution and variance homogeneity. The trueness values were analyzed for the effects of the post-space depth and the scanner type by means of the two-way analysis of variance (ANOVA), followed by Tukey’s post-hoc test. The comparison of the post-scan length with the post-space depth was performed utilizing the one-sample t test. The correlation between trueness and the post-scan length was analyzed using Spearman’s rank-order correlation coefficient. Intergroup comparisons utilized the one-way ANOVA, followed by Tukey’s post-hoc test. The significance level was set at $p < 0.05$ for all tests.

Results

Table 2 presents the significant effects of both the post-space depth and the scanner type on the RMS values ($p = 0.009$ and $p < 0.001$, respectively), though the interaction between the independent variables had no significant effect ($p = 0.178$).

Significant differences were found between the scanners in terms of RMS values ($p < 0.001$). The highest RMS value for trueness was found with CS 3600 (0.30 ± 0.11 mm), followed by Primescan AC (0.26 ± 0.09 mm), while the lowest value was found with Medit i500 (0.18 ± 0.05 mm). In addition, the samples with 8-millimeter-deep post spaces had a significantly higher RMS value than those with 10-millimeter-deep post spaces (0.28 ± 0.10 mm and 0.21 ± 0.09 mm, respectively) ($p = 0.009$).

The post-hoc pairwise comparisons showed that the RMS trueness value was significantly lower for Medit i500 as compared to other scanners ($p < 0.001$).

The intergroup comparisons of the RMS values for trueness, presented in Table 3 and Fig. 5, showed significant differences in the RMS values between different groups ($p < 0.001$). The highest value was found for the CS 3600 group 8 (0.33 ± 0.09 mm), followed by the Primescan AC group 8 (0.31 ± 0.07 mm), the CS 3600 group 10 (0.26 ± 0.11 mm), and the Primescan AC group 10 (0.20 ± 0.07 mm). The lowest values were found for the Medit i500 group 8 (0.18 ± 0.03 mm) and group 10 (0.18 ± 0.06 mm).

Table 2. Two-way ANOVA results for the root mean square (RMS) values for trueness

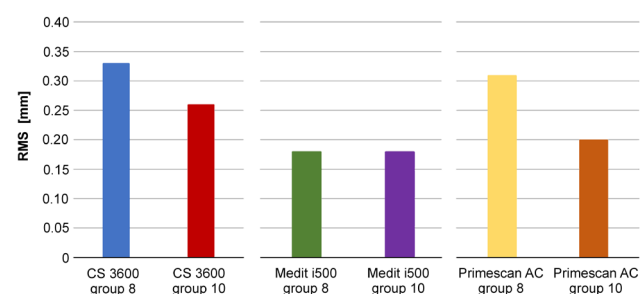
Parameter	Sum of squares	df	Mean square	F -value	p -value
Post-space depth	0.05	1	0.05	7.48	0.009*
Scanner type	0.11	2	0.06	9.42	<0.001*
Post-space depth and scanner type	0.02	2	0.01	1.80	0.178
Error	0.26	42	0.01	–	–

df – degrees of freedom; * statistically significant ($p < 0.05$).

Table 3. Intergroup comparisons in terms of root mean square (RMS) values for trueness

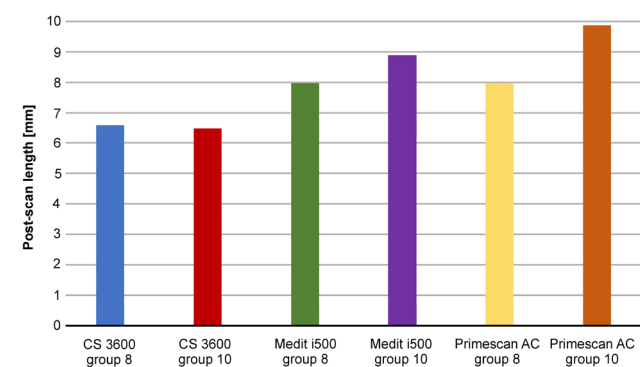
Parameter	Group						<i>p</i> -value
	CS 3600 group 8	Medit i500 group 8	Primescan AC group 8	CS 3600 group 10	Medit i500 group 10	Primescan AC group 10	
RMS [mm]	0.33 ± 0.09 ^a	0.18 ± 0.03 ^c	0.31 ± 0.07 ^{a,b}	0.26 ± 0.11 ^{b,c}	0.18 ± 0.06 ^c	0.20 ± 0.07 ^{b,c}	<0.001*

Data presented as mean ± standard deviation (*M* ± *SD*). * statistically significant (*p* < 0.05); different superscript letters mean statistically significant differences.

**Fig. 5.** Bar chart showing the intergroup comparisons in terms of root mean square (RMS) values for trueness

The post-hoc pairwise comparisons showed that the CS 3600 group 8 had a significantly higher RMS value than all other groups (*p* < 0.001), except for the Primescan AC group 8. In addition, they showed that the Primescan AC group 8 had a significantly higher RMS value than the Medit i500 groups 8 and 10 (*p* < 0.001).

The *M* ± *SD* values for the post-scan length in different groups are shown in Fig. 6. The one-sample *t* test results presented in Tables 4 and 5 show that only for CS 3600, for both the 8 mm and 10 mm post-space depths, there was a significant difference between the post-space depth and the post-scan length (*p* < 0.05).

**Fig. 6.** Bar chart showing the mean values of the post-scan length in different groups**Table 4.** Comparisons of the post-scan length with the post-space depth (8 mm) in different groups

Post-space depth	Scanner	MD (95% CI)	df	<i>t</i> -value	<i>p</i> -value
8 mm	CS 3600	−1.42 (−2.35, −0.48)	7	3.60	0.009*
	Medit i500	−0.03 (−0.05, 0.02)	7	2.17	0.066
	Primescan AC	−0.04 (−0.13, 0.06)	7	0.88	0.404

MD – mean difference; CI – confidence interval; * statistically significant (*p* < 0.05).

Table 5. Comparisons of the post-scan length with the post-space depth (10 mm) in different groups

Post-space depth	Scanner	MD (95% CI)	df	<i>t</i> -value	<i>p</i> -value
10 mm	CS 3600	−3.53 (−4.30, −2.75)	7	10.81	<0.001*
	Medit i500	−1.11 (−2.36, 0.14)	7	2.10	0.074
	Primescan AC	−0.12 (−0.34, 0.11)	7	1.19	0.272

* statistically significant (*p* < 0.05).

Discussion

Accessibility is generally hindered when scanning an intra-coronal restoration design, such as an inlay, as compared to extracoronary designs; it poses a great problem especially in the case of intraradicular preparations.³⁸ The present study involved the scanning of 2 post-space depths of 8 mm and 10 mm with the use of 3 IOSs, and evaluated the trueness of the devices against a reference extraoral five-axis InEos X5 desktop scanner. The accuracy of its results was verified to be within 2.1 μm, according to ISO 12836:2015.^{39–43}

This in vitro study investigated 3 IOSs using different imaging techniques. Primescan AC represents video-rate confocal microscopy, Medit i500 uses video-type scanning based on the triangulation technology and CS 3600 uses video-type scanning active triangulation. All the techniques acquire images with the aid of light and do not require surface coating with powder.⁴⁴

The obtained results necessitated the rejection of the null hypothesis, as they showed significant differences in the trueness of IOSs. Regarding the RMS values, they were higher at 8 mm than at 10 mm, and higher trueness was acquired at the 10 mm depth only in the case of the CS 3600 scanner. A tapered post drill was used for creating post spaces, so the longer the post space, the wider the entrance. This may have led to an increased amount of IOS light entering the post space.¹ Moreover, the CS 3600 scanner had a low scanning depth, which the manufacturer assumed to be up to 12 mm, as compared to the 20 mm for Primescan AC and a range of 12–21 mm (a default depth of 18.5 mm) for Medit i500.^{45–47} The scanning depth was assumed to affect both the feasibility of scanning and the accuracy of the scan data. Besides, the use of low-scanning-depth IOSs is related to a long learning curve, since the operator has to keep a distance from the scanned teeth while watching a computer display. When the maximum depth the IOS can reach

is shallow, image acquisition may not be possible in narrow post-space preparations.³² These findings disagree with a study of Gurpinar and Tak, who investigated and compared the accuracy of different IOSs for scanning different pulpal chamber extension depths, and concluded that deep pulpal chamber extensions of endocrown restorations could negatively affect scanning accuracy.⁴⁸ Moreover, Pinto et al. concluded that the scanning effectiveness of the 3Shape IOS was insufficient for post-space impressions, especially for narrow root canals.¹

Noticeable and significant differences were found for the RMS values between the scanners, regarding the trueness of the captured data. The CS 3600 scanner displayed the highest RMS value and the lowest trueness, while Medit i500 showed higher trueness, followed by Primescan AC. This could be attributed to the different scanning technologies, designs, techniques, and light intensity of each IOS system. The CS 3600 scanner uses a video sequence system, while Medit i500 stitches images. Meanwhile, Primescan AC has been described to use high-frequency contrast analysis as a patent scanning principle. However, various scanning strategies are not clearly explained by the manufacturers.⁴⁹

As a clinically appropriate cement layer thickness has been established to be between 250 µm and 500 µm,⁵⁰ and all the IOSs investigated in this study showed RMS values ≤330 µm, the cement layer was considered clinically acceptable in all cases.

Regarding the post-space depth scans, the results showed significant differences for 8 mm and 10 mm, with the greatest mean difference between the post-scan length and the post-space depth in the case of CS 3600, for both group 8 and group 10. One of the main factors affecting full-depth recording and the trueness of the IOS is the capture box, which is the area in the scanner tip that captures the scanned object in each image. All IOSs require the projection of a sufficient amount of light to the point of interest before it is reflected and recorded. Therefore, a large capture box is preferred for the light to reach deeply for long post-space preparations, as a small capture box requires more stitching or connecting image files, which results in more errors.⁵¹ The field of view was the smallest in CS 3600 (13 mm × 13 mm), as compared to Primescan AC (16 mm × 16 mm) and Medit i500 (14 mm × 13 mm).^{45–47} The results are in agreement with Elter et al., who concluded that Primescan AC could capture a digital post-space impression when the drilled post-space depth was less than 14 mm.⁵²

Other factors influencing trueness, such as the operator's scanning skill, software and illumination, were not considered in this study. The fabrication and the assessment of the fit of the final restorations were also not performed, which might be considered a study limitation.

As the trueness of digital post-space impressions seems to be influenced by the geometry of the post space and the scanner type, Medit i500 and Primescan AC

are preferable when recording the full length of the post-space depth to an acceptable degree in clinical practice; in the case of CS 3600, the discrepancy between the post-scan length and the post-space depth was too large, and the trueness RMS value was too high for the scanner to be clinically accepted.

Conclusions

The Medit i500 scanner showed the highest post-space digital impression trueness as compared to Primescan AC and CS 3600. In the digital impressions captured with the CS 3600, the 10 mm post-space depth had higher trueness than the 8 mm depth. Furthermore, CS 3600 showed less ability to capture the full length of both the 8 mm and 10 mm post-space depths than Primescan AC and Medit i500.

Ethics approval and consent to participate

The study was approved by the ethics committee at the Faculty of Dentistry of the Ain Shams University, Cairo, Egypt (FDASU-REC ER032238). All the procedures applied in the current study were performed in accordance with the relevant guidelines and regulations.

Data availability


The datasets used during the current study are available from the corresponding author on reasonable request.


Consent for publication

Not applicable.

ORCID iDs

Marwa Emam  <https://orcid.org/0000-0003-0856-0689>

Lomaya Ghanem  <https://orcid.org/0000-0003-4258-9346>

Hoda M. Abdel Sadek  <https://orcid.org/0000-0001-7339-0861>

References

1. Pinto A, Arcuri L, Carosi P, et al. In vitro evaluation of the post-space depth reading with an intraoral scanner (IOS) compared to a traditional silicon impression. *Oral Implantol (Rome)*. 2017;10(4):360–368. doi:10.11138/orl/2017.10.4.360
2. Gomes GM, Gomes OM, Gomes JC, Loguerio AD, Calixto AL, Reis A. Evaluation of different restorative techniques for filling flared root canals: Fracture resistance and bond strength after mechanical fatigue. *J Adhes Dent*. 2014;16(3):267–276. doi:10.3290/j.jad.a31940
3. Baba NZ, Goodacre CJ, Daher T. Restoration of endodontically treated teeth: The seven keys to success. *Gen Dent*. 2009;57(6):596–603. PMID:19906612.
4. Morgano SM, Rodrigues AH, Sabrosa CE. Restoration of endodontically treated teeth. *Dent Clin*. 2004;48(2):397–416. doi:10.1016/j.cden.2003.12.011
5. Christopher VS, Ranjan M. Prevalence of age and sex in uses of custom made cast post in endodontically treated teeth – a retrospective study. *Int J Dentistry Oral Sci*. 2021;8(7):3257–3262. doi:10.19070/2377-8075-21000663

6. Berrendero S, Salido MP, Ferreiroa A, Valverde A, Pradíes G. Comparative study of all-ceramic crowns obtained from conventional and digital impressions: Clinical findings. *Clin Oral Investig*. 2019;23(4):1745–1751. doi:10.1007/s00784-018-2606-8
7. Christensen GJ. Impressions are changing: Deciding on conventional, digital or digital plus in-office milling. *J Am Dent Assoc*. 2009;140(10):1301–1304. doi:10.14219/jada.archive.2009.0054
8. Joda T, Zarone F, Ferrari M. The complete digital workflow in fixed prosthodontics: A systematic review. *BMC Oral Health*. 2017;17(1):124. doi:10.1186/s12903-017-0415-0
9. Güth JF, Keul C, Stimmelmayer M, Beuer F, Edelhoff D. Accuracy of digital models obtained by direct and indirect data capturing. *Clin Oral Investig*. 2013;17(4):1201–1208. doi:10.1007/s00784-012-0795-0
10. Pang J, Feng C, Zhu X, et al. Fracture behaviors of maxillary central incisors with flared root canals restored with CAD/CAM integrated glass fiber post-and-core. *Dent Mater J*. 2019;38(1):114–119. doi:10.4012/dmj.2017-394
11. Lee JH. Fabricating a custom zirconia post-and-core without a post-and-core pattern or a scan post. *J Prosthet Dent*. 2018;120(2):186–189. doi:10.1016/j.prosdent.2017.10.004
12. Libonati A, Di Taranto V, Gallusi G, Montemurro E, Campanella V. CAD/CAM customized glass fiber post and core with digital intraoral impression: A case report. *Clin Cosmet Investig Dent*. 2020;12:17–24. doi:10.2147/CCIDE.S237442
13. Yilmaz H, Aydin MN. Digital versus conventional impression method in children: Comfort, preference and time. *Int J Paediatr Dent*. 2019;29(6):728–735. doi:10.1111/ipd.12566
14. Tomita Y, Uechi J, Konno M, Sasamoto S, Iijima M, Mizoguchi I. Accuracy of digital models generated by conventional impression/plaster-model methods and intraoral scanning. *Dent Mater J*. 2018;37(4):628–633. doi:10.4012/dmj.2017-208
15. Jivănescu A, Bara A, Faur AB, Rotar RN. Is there a significant difference in accuracy of four intraoral scanners for short-span fixed dental prosthesis? A comparative in vitro study. *Appl Sci*. 2021;11(18):8280. doi:10.3390/app11188280
16. Wiranto MG, Engelbrecht WP, Tutein Nolthenius HE, van der Meer WJ, Ren Y. Validity, reliability, and reproducibility of linear measurements on digital models obtained from intraoral and cone-beam computed tomography scans of alginate impressions. *Am J Orthod Dentofacial Orthop*. 2013;143(1):140–147. doi:10.1016/j.ajodo.2012.06.018
17. Flügge TV, Schlager S, Nelson K, Nahles S, Metzger MC. Precision of intraoral digital dental impressions with iTero and extraoral digitization with the iTerio and a model scanner. *Am J Orthod Dentofacial Orthop*. 2013;144(3):471–478. doi:10.1016/j.ajodo.2013.04.017
18. Hayashi K, Sachdeva AU, Saitoh S, Lee SP, Kubota T, Mizoguchi I. Assessment of the accuracy and reliability of new 3-dimensional scanning devices. *Am J Orthod Dentofacial Orthop*. 2013;144(4):619–625. doi:10.1016/j.ajodo.2013.04.021
19. Aragón ML, Pontes LF, Bichara LM, Flores-Mir C, Normando D. Validity and reliability of intraoral scanners compared to conventional gypsum models measurements: A systematic review. *Eur J Orthod*. 2016;38(4):429–434. doi:10.1093/ejo/cjw033
20. Anh JW, Park JM, Chun YS, Kim M, Kim M. A comparison of the precision of three-dimensional images acquired by 2 digital intraoral scanners: Effects of tooth irregularity and scanning direction. *Korean J Orthod*. 2016;46(1):3–12. doi:10.4041/kjod.2016.46.1.3
21. Grünheid T, McCarthy SD, Larson BE. Clinical use of a direct chair-side oral scanner: An assessment of accuracy, time, and patient acceptance. *Am J Orthod Dentofacial Orthop*. 2014;146(1):673–682. doi:10.1016/j.ajodo.2014.07.023
22. Naidu D, Freer TJ. Validity, reliability, and reproducibility of the iOC intraoral scanner: A comparison of tooth widths and Bolton ratios. *Am J Orthod Dentofacial Orthop*. 2013;144(2):304–310. doi:10.1016/j.ajodo.2013.04.011
23. Moustapha G, AlShwaimi E, Silwadi M, Ounsi H, Ferrari M, Salameh Z. Marginal and internal fit of CAD/CAM fiber post and cores. *Int J Comput Dent*. 2019;22(1):45–53. PMID:30848254.
24. Jafarian Z, Moharrami M, Sahebi M, Alikhasi M. Adaptation and retention of conventional and digitally fabricated posts and cores in round and oval-shaped canals. *Int J Prosthodont*. 2020;33(1):91–98. doi:10.11607/ijp.6313
25. Våg J, Renne W, Revell G, et al. The effect of software updates on the trueness and precision of intraoral scanners. *Quintessence Int*. 2021;52(7):636–644. doi:10.3290/j.qi.b1098315
26. Nedelcu R, Olsson P, Nyström I, Thor A. Finish line distinctness and accuracy in 7 intraoral scanners versus conventional impression: An in vitro descriptive comparison. *BMC Oral Health*. 2018;18(1):27. doi:10.1186/s12903-018-0489-3
27. Hayama H, Fueki K, Wadachi J, Wakabayashi N. Trueness and precision of digital impressions obtained using an intraoral scanner with different head size in the partially edentulous mandible. *J Prosthodont Res*. 2018;62(3):347–352. doi:10.1016/j.jpor.2018.01.003
28. Kim MK, Kim JM, Lee YM, Lim YJ, Lee SP. The effect of scanning distance on the accuracy of intra-oral scanners used in dentistry. *Clin Anat*. 2019;32(3):430–438. doi:10.1002/ca.23334
29. Larson TD, Nielsen MA, Brackett WW. The accuracy of dual-arch impressions: A pilot study. *J Prosthet Dent*. 2002;87(6):625–627. doi:10.1067/mpr.2002.125180
30. Lim JH, Park JM, Kim M, Heo SJ, Myung JY. Comparison of digital intraoral scanner reproducibility and image trueness considering repetitive experience. *J Prosthet Dent*. 2018;119(2):225–232. doi:10.1016/j.prosdent.2017.05.002
31. Mennito AS, Evans ZP, Lauer AW, Patel RB, Ludlow ME, Renne WG. Evaluation of the effect scan pattern has on the trueness and precision of six intraoral digital impression systems. *J Esthet Restor Dent*. 2018;30(2):113–118. doi:10.1111/jerd.12371
32. Park JM. Comparative analysis on reproducibility among 5 intraoral scanners: Sectional analysis according to restoration type and preparation outline form. *J Adv Prosthodont*. 2016;8(5):354–362. doi:10.4047/jap.2016.8.5.354
33. Park GH, Son K, Lee KB. Feasibility of using an intraoral scanner for a complete-arch digital scan. *J Prosthet Dent*. 2019;121(5):803–810. doi:10.1016/j.prosdent.2018.07.014
34. Neshandar Asli H, Babaee Hemmati Y, Falahchai M. Three-dimensional accuracy of innovative implant-level impression techniques with plastic snap-on impression copings. *Dent Med Probl*. 2021;58(3):351–357. doi:10.17219/dmp/130089
35. Leven R, Schmidt A, Binder R, et al. Accuracy of digital impression taking with intraoral scanners and fabrication of CAD/CAM posts and cores in a fully digital workflow. *Materials (Basel)*. 2022;15(12):4199. doi:10.3390/ma15124199
36. Ashraf Y, Sabet A, Hamdy A, Ebeid K. Influence of preparation type and tooth geometry on the accuracy of different intraoral scanners. *J Prosthodont*. 2020;29(9):800–804. doi:10.1111/jopr.13202
37. Michelinakis G, Apostolakis D, Tsagarakis A, Kourakis G, Pavlakis E. A comparison of accuracy of 3 intraoral scanners: A single-blinded in vitro study. *J Prosthet Dent*. 2019;124(5):581–588. doi:10.1016/j.prosdent.2019.10.023
38. Waldecker M, Rues S, Rammelsberg P, Bömicke W. Accuracy of complete-arch intraoral scans based on confocal microscopy versus optical triangulation: A comparative in vitro study. *J Prosthet Dent*. 2020;126(3):414–420. doi:10.1016/j.prosdent.2020.04.019
39. Kim JE, Hong YS, Kang YJ, Kim JH, Shim JS. Accuracy of scanned stock abutments using different intraoral scanners: An in vitro study. *J Prosthodont*. 2019;28(7):797–803. doi:10.1111/jopr.13095
40. Park JM, Kim RJY, Lee KW. Comparative reproducibility analysis of 6 intraoral scanners used on complex intracoronal preparations. *J Prosthet Dent*. 2020;123(1):113–120. doi:10.1016/j.prosdent.2018.10.025
41. ISO 12836:2015. 2022. <https://www.iso.org/standard/68414.html>. Accessed October 16, 2022.
42. Dentsply Sirona. <https://www.dentsplysirona.com/en-us/categories/lab/cad-cam-equipment-dental-lab/scan.html#technical-data>. Accessed December 22, 2022.
43. Nulty AB. A comparison of full arch trueness and precision of nine intra-oral digital scanners and four lab digital scanners. *Dent J (Basel)*. 2021;9(7):75. doi:10.3390/dj9070075
44. Kim RJY, Benic GI, Park JM. Trueness of ten intraoral scanners in determining the positions of simulated implant scan bodies. *Sci Rep*. 2021;11(1):2606. doi:10.1038/s41598-021-82218-z
45. Dentsply Sirona. <https://news.dentsplysirona.com/en/solutions-topics/primescan.html>. Accessed November 6, 2022.
46. Medit Help Center. <https://support.medit.com/hc/en-us/articles/360039964711-Adjusting-scan-depth>. Accessed November 6, 2022.

47. Carestream 3600 Family Brochure. https://issuu.com/ozonecreative/docs/sua4078_cs3600usfamilybrochure. Accessed December 16, 2022.
48. Gurpinar B, Tak O. Effect of pulp chamber depth on the accuracy of endocrown scans made with different intraoral scanners versus an industrial scanner: An in vitro study. *J Prosthet Dent*. 2020;127(3):430–437. doi:10.1016/j.prosdent.2020.08.034
49. Shin SH, Yu HS, Cha JY, Kwon JS, Hwang CJ. Scanning accuracy of bracket features and slot base angle in different bracket materials by four intraoral scanners: An in vitro study. *Materials (Basel)*. 2021;14(2):365. doi:10.3390/ma14020365
50. Assif D, Bleicher S. Retention of serrated endodontic posts with a composite luting agent: Effect of cement thickness. *J Prosthet Dent*. 1986;56(6):689–691. doi:10.1016/0022-3913(86)90145-9
51. Amornvit P, Rokaya D, Peampring C, Sanohkan S. Confocal 3D optical intraoral scanners and comparison of image capturing accuracy. *Comput Mater Contin*. 2021;66(1):303–314. doi:10.32604/cmc.2020.011943
52. Elter B, Diker B, Tak Ö. The trueness of an intraoral scanner in scanning different post space depths. *J Dent*. 2022;127:104352. doi:10.1016/j.jdent.2022.104352